Old carbon reservoirs were not important in the deglacial methane budget

Published Nature 21 Feb 2020

Permafrost and methane hydrates are large, climate-sensitive old carbon reservoirs that have the potential to emit large quantities of methane, a potent greenhouse gas, as the Earth continues to warm. We present ice core isotopic measurements of methane ($\Delta\,^{14}C$, $\delta\,^{13}C$, and δD) from the last deglaciation, which is a partial analog for modern warming. Our results show that methane emissions from old carbon reservoirs in response to deglacial warming were small (<19 teragrams of methane per year, 95% confidence interval) and argue against similar methane emissions in response to future warming. Our results also indicate that methane emissions from biomass burning in the pre-Industrial Holocene were 22 to 56 teragrams of methane per year (95% confidence interval), which is comparable to today.

M. N. Dyonisius [1] *, V. V. Petrenko [1], A. M. Smith [2], Q. Hua [2], B. Yang [2], J. Schmitt [3], J. Beck [3], B. Seth [3], M. Bock [3], B. Hmiel [1], I. Vimont [4]†, J. A. Menking [5], S. A. Shackleton [6]‡, D. Baggenstos [3,6], T. K. Bauska [5,7], R. H. Rhodes [5,8], P. Sperlich [9], R. Beaudette [6], C. Harth [6], M. Kalk [5], E. J. Brook [5], H. Fischer [3], J. P. Severinghaus [6], R. F. Weiss [6]

Methane (CH_4) is an important contributor to the greenhouse effect, with a global warming potential ~28 times higher than that of carbon dioxide (CO_2) on a 100-year time scale . Natural CH_4 emissions currently account for ~40% of total emissions and there are considerable uncertainties in their response to future warming Although wetlands are the dominant natural source of CH_4, increased emissions from large, climate-sensitive old carbon reservoirs such as permafrost and hydrates under ice sheets might become important in the coming century. Marine hydrates may also have the potential to emit a substantial amount of CH_4 into the atmosphere in response to warming but the time scale of marine hydrate dissociation is relatively long (on the order of hundreds to thousands of years). Furthermore, there is a growing consensus

that CH_4 release to the atmosphere from dissociating marine hydrates will be buffered by efficient CH_4 oxidation in the sediments and water column (

The last deglaciation [18 to 8 kilo-annum before present (ka BP)] provides the opportunity for evaluating the long-term sensitivity of these old carbon reservoirs (marine hydrates, permafrost, and hydrates under ice sheets) to a changing climate. There is abundant evidence of the destabilization of marine hydrates land permafrost degradation and thermokarst lake (permafrost thaw lake) formation during the last deglaciation. However, CH_4 emissions from these old carbon reservoirs into the atmosphere are not well constrained. The paleoatmospheric CH_4 mole fraction and its isotopic composition from trapped air in ice cores provide a historical perspective on how natural CH_4 sources respond to climate change (e.g., Measurements of carbon-14 (^{14}C) of CH_4 ($^{14}CH_4$) from ice cores specifically provide an unambiguous top-down constraint on the globally integrated ^{14}C-free CH_4 emissions from all old carbon reservoirs.

^{14}C decays radioactively and is thus strongly depleted in carbon reservoirs that have been isolated from the atmosphere for time periods longer than its half-life of ~5730 years. Because of the low abundance of ^{14}C (on the order of 10^{-12} compared with ^{12}C), measurements of $^{14}CH_4$ in ice cores are challenging, requiring ~1000 kg of ice per sample. We collected ice cores from a well-dated ice ablation site on Taylor Glacier, Antarctica), which provides easy access to large volumes of old ice at shallow depths. Petrenko *et al.*) recently presented measurements of paleoatmospheric $^{14}CH_4$ from Taylor Glacier for the Younger Dryas–Preboreal (YD-PB) transition (11.7 to 11.3 ka BP) and concluded that ^{14}C-free CH_4 emissions were small [<7.7% of total CH_4 emissions, 95% confidence interval (CI)]. However, their results only spanned a brief time interval within the deglacial transition. In this study, we present 11 additional measurements of paleoatmospheric $^{14}CH_4$ (Fig. 1A) combined with stable isotope measurements ($\delta^{13}CH_4$ and $\delta D\text{-}CH_4$) (Fig. 1, C and D) in the 15- to 8-ka BP time interval, providing a more complete picture of the deglacial CH_4 budget.

The Oldest Dryas–Bølling (OD-B) transition (14.6 to 14.45 ka BP) represents the first large and abrupt CH_4 rise during the last deglacial sequence of events

(Fig. 1B) at the time when sea level was ~100 m lower than today. This abrupt CH_4 rise was synchronous with the acceleration of Northern Hemisphere (NH) warming (Fig. 1E), ice sheet retreat, and rapid sea-level. This climate transition may have also coincided with the first instance of marine hydrate destabilization during the last deglaciation caused by hydrostatic pressure relief from NH ice sheet retreat and incursion of warm intermediate ocean water into shallow, hydrate-bearing Arctic sediment. During the destabilization of marine hydrate reservoirs, abrupt events such as submarine landslides or collapse of marine hydrate pingos could result in large and rapid CH_4 expulsions that may have contributed to the rapid atmospheric CH_4 rise if they were capable of bypassing oxidation in the water column.

In contrast to old carbon reservoirs, contemporaneous CH_4 sources such as wetlands and biomass burning emit CH_4 with a ^{14}C signature that reflects the contemporaneous $\Delta^{14}CO_2$ at the time .Our $\Delta^{14}CH_4$ measurements for the OD-B transition are all within 1σ uncertainty of the contemporaneous atmospheric $\Delta^{14}CO_2$ (Fig. 1A), indicating a dominant role of contemporaneous CH_4 sources. We used a one-box model (see section 4.2 of the materials and methods) to calculate the amount of ^{14}C-free CH_4 emission into the atmosphere (Table 1, fig. S9, and table S10) Our box model shows that the total ^{14}C-free CH_4 emissions during the OD-B transition were small [on average, <13 tera-grams (Tg) of CH_4 per year, 95% CI upper limit]. Combined with earlier $\Delta^{14}CH_4$ data from the YD-PB transition our results argue strongly against the hypothesis regarding old carbon reservoirs being important contributors to the rapid CH_4 increases associated with abrupt warming events (Dansgaard–Oeschger events) This conclusion is consistent with previous studies showing no major enrichment in the CH_4 deuterium/hydrogen ratio (δD-CH_4) concurrent with the abrupt CH_4 transitions (CH_4 from marine hydrates is relatively enriched in δD). It has been shown that even at a relatively shallow water depth of ~30 m, ~90% of the ^{14}C-free CH_4 released from thawing subsea permafrost was oxidized in the water column We hypothesize that during the OD-B transition, relatively rapid sea-level rise associated with meltwater pulse 1-A combined with CH_4 oxidation in the water column may have prevented CH_4 emissions from disintegrating marine hydrates and sub-sea permafrost from reaching the atmosphere.

Our measurements of $^{14}CH_4$ during the Bølling–Allerød interstadial (14.45 to 13 ka BP) and the early Holocene (10 to 8 ka BP) warm period (Fig. 1A) provide an opportunity to assess the likelihood of delayed CH_4 emissions from old carbon reservoirs in response to warming. The onset of marine hydrate dissociation might lag the initial warming signal on decadal centennial, or even millennial time scales. Permafrost degradation could also lag a warming signal on decadal and centennial time scales depending on local environmental conditions such as permafrost depth, soil types, and moisture content During parts of the early Holocene, Arctic temperatures were likely warmer than today providing a good analog for Arctic conditions in the coming decades. Proxy reconstructions of thermokarst lake initiation and land permafrost degradation suggested a potential increase of CH_4 emissions from these processes during both the Bølling–Allerød interstadial and the early Holocene warm period. However, our $\Delta^{14}CH_4$ measurements (Fig. 1A and Table 1) show no evidence of delayed ^{14}C-free CH_4 emissions after warming. These results are consistent with present-day observations that carbon from thermokarst lakes and permafrost is predominantly emitted in the form of CO_2 rather than CH_4 and that CH_4 emissions from permafrost systems are dominated by relatively contemporaneous carbon

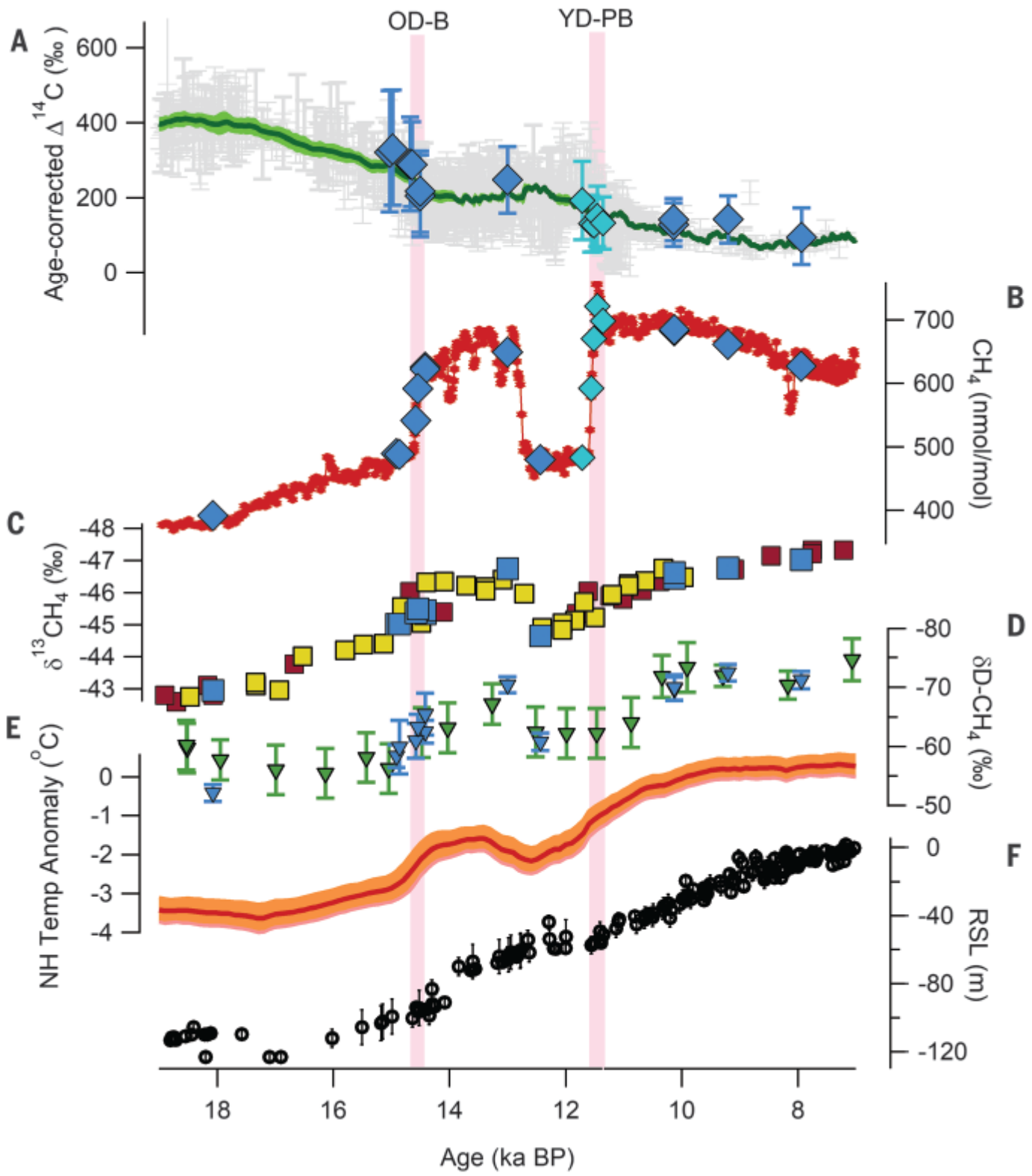

Fig. 1. CH_4 isotopes, mole fraction, NH temperature reconstruction, and relative sea level (RSL) during the last deglaciation. (A) Δ $^{14}CH_4$ from

Taylor Glacier (blue diamonds; this study), Δ ^{14}C of contemporaneous CO $_2$ from Int Cal13 [green line ([19])], Int Cal13 raw data [gray crosses ([19])], and earlier Δ ^{14}CH $_4$ results [light blue diamonds ([15])]. Two Δ ^{14}CH $_4$ samples from the 2014–2015 field season (at 17.8 and 12.8 ka BP) were rejected because of suspected addition of extraneous ^{14}C [see section 3 of the materials and methods ([20])]. (**B**) CH $_4$ mole fraction from discrete WAIS Divide ice core measurements [red dots ([39])], Taylor Glacier (blue diamonds; this study), and an earlier Taylor Glacier study [light blue diamonds ([15])]. (**C**) δ ^{13}CH $_4$ from TALDICE (red squares), EDML [yellow squares ([13])], and Taylor Glacier (blue squares; this study). (**D**) δD-CH $_4$ from EDML [green triangles ([13])] and Taylor Glacier (blue triangles; this study). (**E**) Composite NH temperature stack (red line) and its 95% CI (shaded orange area) ([16]). (**F**) Global RSL inferred from coral data ([32]). All ice core data are plotted with respect to the WD2014 age scale ([40]); IntCal13, RSL, and NH temperature stacks are plotted on their respective age scales. All error bars represent the 95% CI.

Viewable Image - nh temperature reconstructio

Image Caption

Fig. 1. CH_4 isotopes, mole fraction, NH temperature reconstruction, and relative sea level (RSL) during the last deglaciation. (**A**) Δ ^{14}CH $_4$ from Taylor Glacier (blue diamonds; this study), Δ ^{14}C of contemporaneous CO $_2$ from Int Cal13 [green line ([19])], Int Cal13 raw data [gray crosses ([19])], and earlier Δ ^{14}CH $_4$ results [light blue diamonds ([15])]. Two Δ ^{14}CH $_4$ samples from the 2014–2015 field season (at 17.8 and 12.8 ka BP) were rejected because of suspected addition of extraneous ^{14}C [see section 3 of the materials and methods ([20])]. (**B**) CH $_4$ mole fraction from discrete WAIS Divide ice core measurements [red dots ([39])], Taylor Glacier (blue diamonds; this study), and an earlier Taylor Glacier study [light blue diamonds ([15])]. (**C**) δ ^{13}CH $_4$ from TALDICE (red squares), EDML [yellow squares ([13])], and Taylor Glacier (blue squares; this study). (**D**) δD-CH $_4$ from EDML [green triangles ([13])] and Taylor Glacier (blue triangles; this study). (**E**) Composite NH temperature stack (red line) and its 95% CI (shaded orange area) ([16]). (**F**) Global RSL inferred from coral data ([32]). All ice core data are plotted with respect to the WD2014 age scale ([40]); IntCal13, RSL, and NH temperature stacks are plotted on their respective age scales. All error bars represent the 95% CI.

Because carbon stored in permafrost is not expected to be ^{14}C free we also attempted to use our $^{14}CH_4$ results to calculate the possible magnitude of CH_4 emissions from thawing old carbon in permafrost (Section 4.3) This calculation assumed that the ^{14}C activity of permafrost CH_4 emissions follows

the predepositional age of terrigenous biomarkers released from thawing permafrost (7500 ± 2500 years old relative to our sample age) Resulting CH_4 emissions from old permafrost carbon range from 0 to 53 Tg CH_4 per year (table S10) throughout the last deglaciation and may have contributed up to 27% of the total CH_4 emissions to the atmosphere (95% CI upper limit) at the end of the OD-B transition (14.42 ka BP). However, we consider this calculation speculative (see section 4.3 of the materials and methods)

When the global sea level was lower, exposure of continental shelves may have resulted in higher CH_4 emissions fromnatural geologic seeps A recent study also inferred the existence of CH_4 hydrate deposits underneath ice sheets and suggested that the proglacial meltwater discharge is likely an important source of CH_4 to the atmosphere Ice sheet retreat during the last deglaciation may have destabilized the subglacial hydrate deposits, which contain old, ^{14}C-depleted CH_4.However, our data, which span most of the deglacial ice retreat and sea-level rise (Fig. 1F), argue strongly against both hypotheses. The ^{14}C-free CH_4 emissions were small throughout the last deglaciation (Table 1) and appear to be insensitive to both global sea level and ice volume.

Biomass burning is an important component of the global carbon cycle and is tightly coupled with emissions of carbon monoxide (CO), nitrogen oxides (NO_x), nonmethane hydrocarbons, and aerosols that have substantial effects on atmospheric chemistry and radiative energy fluxes. Compared with other proxies of past biomass burning, CH_4 has an advantage because it is a well-mixed gas in the atmosphere and can represent the globally integrated biomass-burning emissions. Bock *et al.* provided the most recent stable isotope–based ($\delta^{13}C$ and δD) study of the glacial–interglacial CH_4 budget, but they were unable to separate the relative contributions from CH_4 sources that are enriched in heavier isotopes (biomass burning and natural geologic emissions). With improved estimates of natural geologic emissions, our results allow for better constraints on the overall CH_4 budget. We used the stable isotope data (Fig. 1, C and D) in a one-box model (see section 5 of the materials and methods) (to calculate CH_4 emissions from biomass burning ($CH_{4\ bb}$) and microbial sources ($CH_{4\ mic}$, composed of emissions from wetlands, ruminants, and termites) for the Early Holocene (Table 1 and fig.

S11) We extended our calculation to the late Holocene (~2ka BP) (Table 1) to directly compare our CH_4 source strength estimates with those of earlier studies). This assumption can be justified because a large change in the natural geologic emissions between the early Holocene and 2 ka BP seems unlikely because global sea level and ice volume did not change appreciably after 8 ka BP However, we did not perform this calculation for the pre-Holocene samples because estimates of the CH_4 interpolar difference, atmospheric global average CH_4 stable isotope values, and stable isotopic signatures of the sources are more uncertain (Section 5)

Table 1. CH_4 source strength estimates (95% CI) for the time intervals of our samples. Sample ages were determined by
well-mixed gases (CH_4 and $\delta^{18}O$ of atmospheric oxygen) to WD2014 chronology [see section 1 of the materials and methods (*20*
this table represent the "best" (maximum probability) age on the probability distribution (fig. S3) (*20*) with respect to WD201

Sample name	Sample age (ka BP)	CH_4 mole fraction (nmol/mol)	Age-corrected $\Delta^{14}CH_4$ (‰)	Total source (Tg CH_4/year)	^{14}C-free emissions (Tg CH_4/year)	$CH_{4\ bb}$ em (Tg CH_4
Oldest Dryas 1	14.92	484.5 ± 3.9	317 ± 166	141.3 ± 14.4	0–13	
Oldest Dryas 2	14.86	485.9 ± 3.9	327 ± 151	142.3 ± 14.7	0–10	
Transition 1	14.58	543.0 ± 3.9	288 ± 128	158.8 ± 17.1	0–11	
Transition 2	14.54	584.8 ± 3.9	287 ± 112	164.7 ± 18.8	0–10	
Bølling 2	14.42	624.4 ± 3.9	216 ± 109	178.5 ± 19.5	0–17	
Bølling 1	14.42	621.1 ± 3.9	204 ± 111	177.9 ± 20.1	0–20	
Allerød	13.00	647.2 ± 3.9	246 ± 90	190.2 ± 19.4	0-8	
10.2K1	10.13	681.6 ± 3.9	126 ± 58	206.7 ± 20.7	0–11	32–
10.2K2	10.13	681.6 ± 3.9	139 ± 57	206.7 ± 20.7	0–8	33–
9.2K	9.21	659.7 ± 3.9	141 ± 63	200.4 ± 20.1	0–2	31–
8.2K	7.94	623.9 ± 3.9	92 ± 74	187.8 ± 19.3	0–11	27–
*Late Holocene**	1.95	–	–	171.0 ± 18.8	0–9*	22–

*The ^{14}C-free emissions for this period are extrapolated from the average of ^{14}C-free emissions in the early Holocene (10 to 8 ka BP). This assumption can be
the natural geologic emissions between the early Holocene and 2 ka BP seems unlikely given that the global sea level and ice volume did not change conside
isotopes ($\delta^{13}CH_4$, δD-CH_4) and CH_4 mole fraction from (*11*) at 2 ka BP to calculate the $CH_{4\ bb}$ and $CH_{4\ mic}$ emissions.

We calculated relatively high CH_{4bb} emissions in the early Holocene (33 to 56 Tg CH_4 per year, 95% CI) at 10 ka BP and a slight decrease of CH_{4bb} emissions (22 to 42 Tg CH_4 per year, 95% CI) toward the late Holocene (Table 1). However, the magnitude of the decrease in biomass-burning emissions (~7 Tg CH_4 per year) is small relative to the uncertainties for both the CH_{4bb} and $CH_{4\ mic}$ emissions (±11 and ±18 Tg CH_4 per year, respectively, 95% CI uncertainties). Our estimate of 22 to 42 Tg CH_4 per year (95% CI)

CH_{4bb} emissions for the late Holocene period (~2 ka BP) is within the upper range of estimates from previous ice core studies .Considering the large downward revision of natural geologic emissions inferred from our ^{14}C data, an upward revision in pyrogenic CH_4 emissions is expected to balance the CH_4 stable isotope budget. The increase in $CH_{4\ bb}$ expected from a reduction in natural geologic emissions is partly offset by a –0.5 to –1‰ revision in atmospheric $\delta^{13}CH_4$ values because the $\delta_{13}CH_4$ values from earlier studies were likely biased because of krypton (Kr) interference Our $CH_{4\ bb}$ estimates are also reduced because, unlike previous studies, we accounted for temporal shifts in the isotopic signatures of $CH_{4\ bb}$ and $CH_{4\ mic}$ between the pre-Industrial Holocene and the modern period expected from anthropogenically driven changes in the $\delta^{13}CO_2$ precursor material and land use (see section 5.2 of the materials and methods) . Our best $CH_{4\ bb}$ estimates for the late Holocene (22 to 42 Tg CH_4 per year, 95% CI) are comparable to the present-day estimates of combined pyrogenic CH_4 emissions from anthropogenic biomass burning and wildfires This result is supported by some (but not all independent paleoproxies of biomass burning.

The last deglaciation serves only as a partial analog to current anthropogenic warming, with the most important differences being the much colder baseline temperature, lower sea level, and the presence of large ice sheets covering a large part of what are currently permafrost regions in the NH. Although Arctic temperatures during the peak early Holocene warmth were likely warmer than today they were still lower than the Arctic temperature projections by the end of this century under most warming scenarios However, there are also many similarities between the last deglaciation and current anthropogenic warming. Both deglacial and modern warming include strong Arctic amplification, and the magnitude of global warming (~4°C) during the last deglaciation was comparable to the expected magnitude of equilibrium global temperature change under midrange anthropogenic emission scenarios Because the relatively large global warming of the last deglaciation (which included periods of large and rapid regional warming in the high latitudes) did not trigger CH_4 emissions from old carbon reservoirs, such CH_4 emissions in response to anthropogenic warming also appear to be unlikely. Our results instead support the hypothesis that natural CH_4 emissions involving contemporaneous carbon from wetlands are likely to increase as warming continues We also estimated

relatively high $CH_{4\ bb}$ emissions for the pre-Industrial Holocene that were comparable to present-day combined pyrogenic CH_4 emissions from natural and anthropogenic sources. This result suggests either an underestimation of present-day $CH_{4\ bb}$ or a two-way anthropogenic influence on fire activity during the Industrial Revolution: reduction in wildfires from active fire suppression and landscape fragmentation balanced by increased fire emissions from land-use change (deforestation) and traditional biofuel use (burning of plant materials for cooking and heating).

[1]Department of Earth and Environmental Sciences, University of Rochester, Rochester, NY 14627, USA.
[2]Australian Nuclear Science and Technology Organisation (ANSTO), Lucas Heights, NSW 2234, Australia.
[3]Climate and Environmental Physics, Physics Institute and Oeschger Centre for Climate Change Research, University of Bern, CH-3012 Bern, Switzerland.
[4]Institute of Arctic and Alpine Research, University of Colorado Boulder, Boulder, CO 80303, USA.
[5]College of Earth, Ocean and Atmospheric Sciences, Oregon State University, Corvallis, OR 97331, USA.
[6]Scripps Institution of Oceanography (SIO), University of California, San Diego, La Jolla, CA 92037, USA.
[7]British Antarctic Survey High Cross, Cambridge CB3 0ET, UK.
[8]Department of Earth Sciences, University of Cambridge, Cambridge CB2 3EQ, UK.
[9]National Institute of Water and Atmospheric Research (NIWA), 6021 Wellington, New Zealand.
*Corresponding author. Email: mdyonisi@ur.rochester.edu

†Present address: Cooperative Institute for Research in Earth Sciences, University of Colorado, Boulder, CO 80309, USA.

‡Present address: Department of Geosciences, Princeton University, Princeton, NJ 08544, USA.

1. G. Myhre, D. Shindell, in *Climate Change 2013: The Physical Science Basis. Contribution of Working Group I to the Fifth Assessment Report of the Intergovernmental Panel on Climate Change*, T. F. Stocker *et al*., Eds. (Cambridge Univ. Press, 2013), pp. 659–740.
2. M. Saunois *et al., Earth Syst. Sci. Data* **8**, 697 (2016).
3. J. F. Dean *et al., Rev. Geophys.* **56**, 207–250 (2018).
4. E. A. G. Schuur *et al., Nature* **520**, 171–179 (2015).
5. G. Lamarche-Gagnon *et al., Nature* **565**, 73–77 (2019).
6. M. Maslin *et al., Philos. Trans. A Math. Phys. Eng. Sci.* **368**, 2369–2393 (2010).
7. C. D. Ruppel, J. D. Kessler, *Rev. Geophys.* **55**, 126–168 (2017).
8. K. Andreassen *et al., Science* **356**, 948–953 (2017).
9. J. P. Kennett, K. G. Cannariato, I. L. Hendy, R. J. Behl, in *Methane Hydrates in Quaternary Climate Change: The Clathrate Gun Hypothesis* (American Geophysical Union, 2013).
10. M. Winterfeld *et al., Nat. Commun.* **9**, 3666 (2018).

11. K. M. Walter, M. E. Edwards, G. Grosse, S. A. Zimov, F. S. Chapin 3rd, *Science* **318**, 633–636 (2007).
12. J. Beck *et al., Biogeosciences* **15**, 7155–7175 (2018).
13. M. Bock *et al., Proc. Natl. Acad. Sci. U.S.A.* **114**, E5778–E5786 (2017).
14. D. Baggenstos *et al., Clim. Past* **13**, 943–958 (2017).
15. V. V. Petrenko *et al., Nature* **548**, 443–446 (2017).
16. J. D. Shakun *et al., Nature* **484**, 49–54 (2012).
17. P. Deschamps *et al., Nature* **483**, 559–564 (2012).
18. D. Archer, *Biogeosciences* **4**, 993–1057 (2007).
19. P. J. Reimer *et al., Radiocarbon* **55**, 1869–1887 (2013).
20. Materials and methods are available as supplementary materials.
21. K. J. Sparrow *et al., Sci. Adv.* **4**, eaao4842 (2018).
22. M. Leonte *et al., Geochim. Cosmochim. Acta* **204**, 375–387 (2017).
23. C. Stranne, M. O'Regan, M. Jakobsson, *Geophys. Res. Lett.* **43**, 8703–8712 (2016).
24. A. V. Reyes, C. A. Cooke, *Proc. Natl. Acad. Sci. U.S.A.* **108**, 4748–4753 (2011).
25. B. S. Lecavalier *et al., Proc. Natl. Acad. Sci. U.S.A.* **114**, 5952–5957 (2017).
26. C. D. Elder *et al., Nat. Clim. Chang.* **8**, 166–171 (2018).
27. M. D. A. Cooper *et al., Nat. Clim. Chang.* **7**, 507–511 (2017).
28. P. J. Mann *et al., Nat. Commun.* **6**, 7856 (2015).
29. B. Luyendyk, J. Kennett, J. F. Clark, *Mar. Pet. Geol.* **22**, 591–596 (2005).
30. D. F. Ferretti *et al., Science* **309**, 1714–1717 (2005).
31. C. J. Sapart *et al., Nature* **490**, 85–88 (2012).
32. K. Lambeck, H. Rouby, A. Purcell, Y. Sun, M. Sambridge, *Proc. Natl. Acad. Sci. U.S.A.* **111**, 15296–15303 (2014).
33. J. Schmitt *et al., Atmos. Meas. Tech.* **6**, 1425–1445 (2013).
34. M. R. Nicewonger, M. Aydin, M. J. Prather, E. S. Saltzman, *Proc. Natl. Acad. Sci. U.S.A.* **115**, 12413–12418 (2018).
35. Z. Wang, J. Chappellaz, K. Park, J. E. Mak, *Science* **330**, 1663–1666 (2010).
36. A.-L. Daniau *et al., Global Biogeochem. Cycles* **26**, n/a (2012).
37. M. Collins, R. Knutti, in *Climate Change 2013: The Physical Science Basis. Contribution of Working Group I to the Fifth Assessment Report of the Intergovernmental Panel on Climate Change*, T. F. Stocker *et al*., Eds. (Cambridge Univ. Press, 2013), pp. 1029–1136.
38. P. U. Clark *et al., Abrupt Climate Change: A Report by the US Climate Change Science Program and the Subcommittee on Global Change Research* (U.S. Geological Survey, 2008).
39. WAIS Divide Project Members, *Nature* **520**, 661–665 (2015).
40. M. Sigl *et al., Clim. Past* **12**, 769–786 (2016).

ACKNOWLEDGMENTS

We thank M. Jayred and J. Jetson for ice drilling; camp managers K. Schroeder and C. Llewelyn and field team members A. Palardy and J. Ward for assistance; the U.S. Antarctic Program for logistical support; M. Sigl and F. Adolphi for assistance with age-scale transfer between IntCal13 and WD2014; H. Schaefer for suggestions regarding the isotope box model; G. Mollenhauer for discussions regarding the ^{14}C-age of terrigenous biomarkers; and P. F. Place Jr., M. Diaz, and M. Paccico for help with field gear preparations. **Funding:** This work was supported by NSF awards PLR-

1245659 (V.V.P.), PLR-1245821 (E.J.B), and PLR-1246148 (J.P.S.); the Packard Fellowship for Science and Engineering (V.V.P.); the European Research Council (ERC) under the European Union's Seventh Framework Programme FP7/2007-2013 ERC Grant 226172 [ERC Advanced Grant Modern Approaches to Temperature Reconstructions in Polar Ice Cores (MATRICs); H.F.]; the Swiss National Science Foundation 200020_172506 (H.F.); Australian Government for the Centre for Accelerator Science at ANSTO through the National Collaborative Research Infrastructure Strategy (A.M.S, Q.H., B.Y.); and the National Institute of Water and Atmospheric Research through the Greenhouse Gases, Emissions and Carbon Cycle Science Program (P.S.). **Author contributions:** V.V.P., E.J.B., and J.P.S. designed the study. M.N.D., V.V.P., and B.H. conducted field logistical preparations. M.N.D., V.V.P., J.A.M., S.A.S., B.H., I.V., D.B., T.K.B., P.S., E.J.B., J.P.S., and R.H.R. conducted the field sampling and reconnaissance. M.N.D. extracted CH_4 and CO from air samples. Q.H. and B.Y. graphitized the ^{14}C samples. A.M.S. conducted the 14C measurements. J.B. and B.S. made the CH_4 stable isotopes measurements ($\delta^{13}C$ and $\delta D\text{-}CH_4$) under the supervision of J.S., M.B., and H.F. D.B. and J.P.S. made the Xe/Kr, Kr/N_2, and Xe/N_2 measurements. R.B. made the $\delta^{15}N_2$, $\delta^{18}O_{atm}$, $^{40}Ar/^{36}Ar$, O_2/N_2, and Ar/N_2 measurements. C.H. made the CH_4 mole fraction and halogenated trace gas measurements under the supervision of R.F.W. M.K. made the CH_4 mole fraction and total air content measurements on the ice samples under the supervision of E.J.B. I.V. made the $\delta^{13}CO$ measurement for the CO dilution gas. S.A.S and M.N.D. developed the age scale for the samples. M.N.D. and V.V.P. analyzed the results and wrote the manuscript with input from all authors. **Competing interests:** The authors declare no competing interests. **Data and materials availability:** Data from this work are available through the USAP Data Center: **https://gcmd.nasa.gov/search/Metadata.do?entry=USAP-1245659**.

10.1126/science.aax0504

SUPPLEMENTARY MATERIALS

science.sciencemag.org/content/367/6480/907/suppl/DC1

Materials and Methods Supplementary Text Figs. S1 to S12

Tables S1 to S11

References (*41*–*98*)

19 February 2019; accepted 6 Jan